Journal of Radioanalytical and Nuclear Chemistry (2023) 332:95–104
https://doi.org/10.1007/s10967-022-08708-0

Application of gamma spectrometry for the characterization and influence of the archeological works of an archaeological site

V. M. Expósito-Suárez[1] · J. A. Suárez-Navarro[1] · P. Vacas-Arquero[1] · A. Caro[1]

Received: 11 August 2022 / Accepted: 3 December 2022 / Published online: 25 December 2022

Abstract

The purpose of this study was the use of gamma spectrometry to characterize the archaeological site of Molina de Aragón, located in the province of Guadalajara in Spain. To do so, a set of samples with different historical influences have been selected. The samples were analyzed by gamma spectrometry with HPGe detectors, and by X-ray fluorescence, to know their chemical composition. The statistical study of the activity concentration of radionuclides from the natural radioactive series, ^{40}K and ^{137}Cs, was carried out using box-and-whisker plots, cluster analysis and principal component analysis (PCA). Likewise, the in-situ effective dose rates and the ones determined from the activity concentrations obtained by gamma spectrometry were evaluated to verify sampling reproducibility. The results obtained made it possible to classify the areas of Jewish and Christian influence based on the relationships between ^{232}Th and ^{238}U series and the possible influence of the archaeological works carried out in the study area. The least altered areas could also be identified from the activity concentrations of ^{137}Cs and $^{210}Pb_{ex}$. Activity concentrations and effective dose rates were equivalent to the natural radioactive background of the Iberian Peninsula. PCA showed a correlation between Fe_2O_3, Al_2O_3 y ZrO_2 and the natural radioactive series of thorium and uranium.

Keywords Gamma spectrometry · ^{137}Cs · $^{210}Pb_{ex}$ · Archaeology · Natural radioactive series · HJ-Biplot

Introduction

Historically, Spain has been a country with a very abundant and varied archaeological wealth. In Spain there are remains of different cultures and civilizations such as: cave paintings (Atapuerca, Altamira …), remains of the Bronze Age (Motilla del Azuer, La Codera, …), Arab culture (Medina Azahara, Córdoba, Granada, …), Romans (Tárraco, Itálica, Baelo Claudia, Mérida, …), Visigothics and Islamic remains (Minateda), and a long etcetera. There are also architectural remains from more recent times, between the twelfth and sixteenth centuries, in which Romanesque and Gothic art had its maximum splendour (Segovia, Salamanca…). The period called the Middle Ages, covered the period of time between the fifth and fifteenth centuries, comprising several of the above-mentioned periods. The archaeological study of remains from these cultures is carried out with chemical techniques (XRF, ICP-MS, etc.), used for their characterization and dating [1]. In this sense, the project called ArcheoMedtal arises, which aims to include other types of techniques such as gamma spectrometry to characterize archaeological remains from the Middle Ages.

Gamma spectrometry is a non-destructive technique that allows the determination of the activity concentration of several gamma-emitting radionuclides in a single measurement [2]. Gamma-emitting radionuclides, both natural and artificial, provide valuable information to carry out a characterization of this type of archaeological remains. The possible imbalances between natural radionuclides belonging to the three natural radioactive series of uranium, actinium and thorium allow us to interpret the weathering phenomena that have been able to alter the materials over time [3, 4]. These alterations can be interpreted based on the different chemical and physical properties of these radionuclides [5].

V. M. Expósito-Suárez and J. A. Suárez-Navarro share first authorship in this work.

✉ J. A. Suárez-Navarro
ja.suarez@ciemat.es

[1] Centro de Investigaciones Energéticas, Medioambientales y Tecnológicas (CIEMAT), Avd/ Complutense, 40, 28040 Madrid, Spain

Furthermore, artificial radionuclides such as ^{137}Cs from the fallout are a tool used to study possible ground alterations [6].

In the present work, we set out to evaluate the use of gamma spectrometry as an alternative technique to the existing ones for the physical–chemical characterization of archaeological remains. Our working hypothesis is that the gamma-emitting radionuclides present in the study area, allow characterizing and interpreting the historical footprint that occurred in the archaeological remains belonging to the measured age period. We test our hypothesis by analyzing different samples taken from the ruins of the historic site of Molina de Aragón (Guadalajara province, Spain) to see the possible anthropic prediction derived from the metallurgical work carried out at this site. Soils with productive and non-productive implications were sampled. The objectives of this study were: (1) to characterize the study area using gamma spectrometry, in-situ measurements of the environmental equivalent dose and X-ray fluorescence, and (2) to statistically evaluate the historical footprint of the site and the influence of archaeological works.

Experimental

Study area

The samples analyzed in this work were taken in the Castle of Molina de Aragón and in "Prao de los Judios", located in the historic complex of Molina de Aragón in the province of Guadalajara (Spain). This historical complex combines archaeological remains of the Jewish and Christian cultures during the Middle Ages [7]. The samples were selected to contemplate remains of these two cultures.

Samples 1, 2 and 3 were taken in the inner courtyard of the castle, sample 10 at the base of the Christian church and sample 4 at the hillside. All these samples were located inside the walled enclosure. The area with purely Jewish influence was represented with samples 5–9, which were located outside the walled enclosure. The samples were collected in different dependencies whose uses were: pottery (sample 5), metal foundry (sample 6), livestock activity (sample 7), housing (sample 8) and synagogue (sample 9). Figure 1 shows the different sampling points within the historic complex of Molina de Aragón.

Sample collection and preparation

The minimum quantity necessary of soil samples were collected superficially since it was not allowed to perform alterations in the studied ruins. Sampling was done with a 30 cm × 30 cm grid, taking 5 fractions in the four corners and in the center of the grid. These samples were then bagged and identified. Subsequently, the samples were dried in a Selecta oven at 105 °C. Once constant weight was obteined, the dried samples were ground in a FRITSCH brand ball mill (Planetary Ball Mill, pulverisette 5) and sieved at 300 µm. Finally, samples were deposited in a cylindrical polypropylene box with a diameter of 76 mm and a height of 30 mm. The boxes were completely sealed using parafilm to prevent loss of ^{222}Rn, and were left to rest for 21 days to achieve secular equilibrium between ^{226}Ra and ^{214}Pb and ^{214}Bi.

Gamma spectrometry

In this study, 3 types of gamma detectors were used: (1) extended range coaxial, (2) reverse electrode coaxial and (3) broad energy. Detectors were connected to 3 electronic chains consisting of a high voltage source (HV), an amplifier (AMP), an analog digital converter (ADC) and a data transfer module (AIM), all of them from Canberra Industries brand. The electronic chains were connected to a PC and the spectra were acquired and analyzed using Genie 2000 software. Efficiencies were calculated using LabSOCS software as the 3 detectors were characterized by CANBERRA. To calculate the efficiency, the procedure described was the one developed in [2]. The energies and emission probabilities of the radionuclides analyzed in this study were the following [8]: ^{234}Th (63.30 (2) keV—3.75 (8)%), ^{226}Ra (186.211 (13) keV—3.555 (19)%), ^{214}Pb (351.932 (2) keV—35.60 (7)%), ^{214}Bi (609.312 (7) keV—45.49 (19)%; 1120.287 (10) keV—14.91 (3)%; 1764.494 (14) keV—15.31 (5)%), ^{210}Pb (46.539 (1) keV—4.252 (40)%), ^{212}Pb (238.632 (2) keV—43.6 (5)%), ^{208}Tl (583.187 (2) keV—85.0 (3)%), ^{228}Ac (911.196 (6) keV—26.2 (8)%), ^{235}U (163.356 (3) keV—5.08 (3)%; 205.16 (4) keV—5.02 (3)%; 143.767 (3) keV—10.94 (6)%), ^{40}K (1460.822 (6) keV—10.55 (11)%) and ^{137}Cs (661.657 (3) keV—84.99 (20)%). Interferences of ^{235}U with the 186 keV photopeak of ^{226}Ra, and ^{228}Ac with the 1460 keV photopeak of ^{40}K were corrected using the method proposed in [9].Samples were measured for 80,000 s and the backgrounds were measured for 600,000 s [10].The gamma spectrometry laboratory, where the measurements were performed, is accredited based on the UNE-EN ISO/IEC 17025:2017 standard [11].

Chemical composition of samples

Chemical composition of samples was determined by X-ray fluorescence (WDXRF). An aliquot of each sample was shaped and sieved to 70 µm particle size with a 200 mesh sieve. The analysis was performed in the Chemistry Division of CIEMAT with a Malvern-PAN analytical AXIOS automated spectrometer.

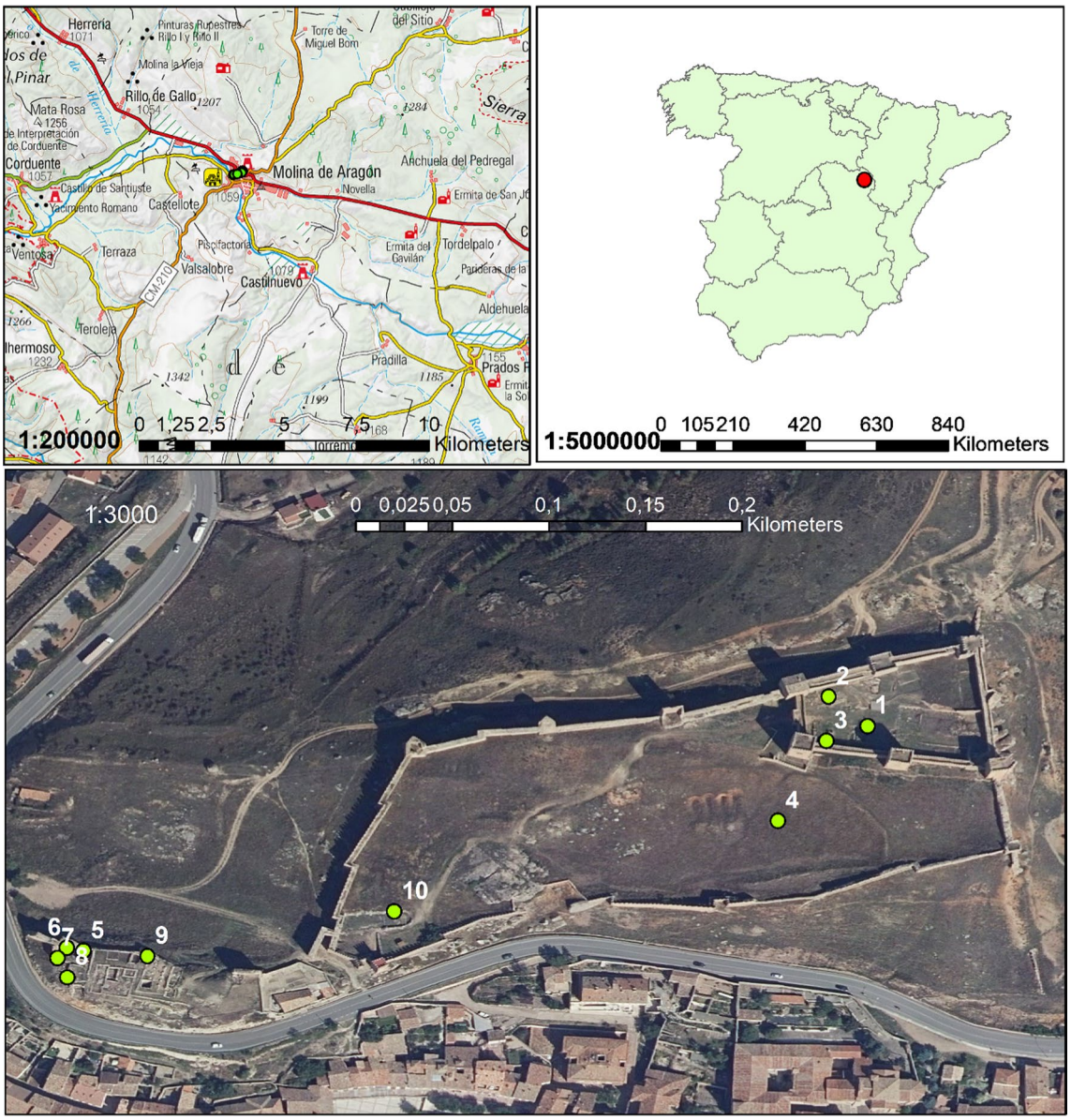

Fig. 1 Location of the sampling points in the historic complex of Molina de Aragón in the province of Guadalajara (Spain)

Absorbed and effective dose rates calculation

Effective dose rates were measured in-situ and calculated from the activity concentrations obtained by gamma spectrometry. In-situ $H^*(10)$ effective dose rates at 1 m above ground were measured using a Lamse model MS6020 portable multi-probe monitor with an RD2L probe. Theoretical effective dose rates were calculated from the absorbed dose, determined using the kerma rate per unit activity at 1 m height (nGy h^{-1} per Bq kg^{-1}) for natural radionuclides (uranium, actinium and thorium series along with ^{40}K) and ^{137}Cs from the fallout [12, 13]. The expression used to calculate the absorbed dose rate at 1 m height ($\dot{D}_{1m}$, nGy h^{-1}) was the following one:

$$\begin{aligned}\dot{D}_{1m} = {} & 5.79 \cdot 10^{-3} \cdot C_{^{234}\mathrm{Th}} + 1.41 \cdot 10^{-3} \cdot C_{^{226}\mathrm{Ra}} \\ & + 5.46 \cdot 10^{-2} \cdot C_{^{214}\mathrm{Pb}} \quad + \cdots + 4.01 \cdot 10^{-1} \cdot C_{^{214}\mathrm{Bi}} \\ & + 3.58 \cdot 10^{-4} \cdot C_{^{210}\mathrm{Pb}} + 2.24 \cdot 10^{-1} \cdot C_{^{228}\mathrm{Ac}} \\ & + \cdots + 5.49 \cdot 10^{-2} \cdot C_{^{212}\mathrm{Pb}} + 3.26 \cdot 10^{-1} \cdot C_{^{208}\mathrm{Tl}} \\ & + 1.25 \cdot 10^{-1} \cdot C_{^{235}\mathrm{U}} + \cdots + 4.17 \cdot 10^{-2} \cdot C_{^{40}\mathrm{K}} \\ & + 1.24 \cdot 10^{-1} \cdot C_{^{137}\mathrm{Cs}}\end{aligned} \quad (1)$$

where $C_{^{xxx}A}$ is the activity concentration in Bq kg^{-1} of radionuclide ^{xxx}A.

The expression used to determine the effective dose rate (E, μSv h^{1}) was as follows:

$$E = \dot{D}_{1m} \cdot O \cdot C \cdot 10^{-3} \quad (2)$$

where O is the occupancy factor that was considered 1 to be compared with the average in-situ $H^*(10)$, C is the conversion factor from absorbed dose in air to effective dose received by an adult (equal to 0.7 Sv Gy^{-1}). The uncertainties associated with expressions (1) and (2) were estimated using the Kargten method [14, 15].

Statistics

Analyses used were: (1) box-and-whisker plots, (2) cluster analysis with the nearest-neighbour method and squared Euclidean distance and (3) relative kurtosis and skewness. This statistical study of the data was performed using the Statgraphics Centurion XVII software, version 17.0.16. The box-and-whisker plot was used to analyze the possible imbalances in the natural radioactive series and the distribution of activity concentrations obtained for ^{40}K. Standardized kurtosis and skewness were used to check whether the activity concentrations of a given radionuclide fit a normal distribution. Cluster analysis was used to search for simple groupings based on their chemical composition and radiological content [16].

Relationship between the activity concentrations of natural (natural series together with ^{40}K) and anthropogenic (^{137}Cs) gamma-emitting radionuclides were analyzed along with chemical composition using principal component analysis. Factors selection was made based on the KMO (Kaiser–Meyer–Olkin) parameter. The analysis was carried out iteratively, removing the factors with the least correlation until a KMO greater than 0.7 was obtained, which indicates an acceptable correlation in the PCA [17]. The PCA analysis for this paper was generated using the Real Statistics Resource Pack software (Release 7.6). Copyright (2013–2021) Charles Zaiontz. www.real-statistics.com [18]. Lastly, variables and scores of the samples were represented using a HJ-Biplot graph [19].

Comparison of in-situ and theoretical dose rates was performed using three statistical tests: (1) overlap percentage, to compare individual values [20], (2) Student's t-test to check if the means were statistically comparable, and (3) Fisher's F to verify if the variances were statistically comparable. Both tests were done for an $\alpha = 0.05$ and for the tails test since it was sought whether the means and variances were statistically comparable, or not [21].

Results

Activity concentrations of the samples from the historic site of Molina de Aragón

Table 1 shows the activity concentrations (Bq kg^{-1}) of the samples collected in the historical site of Molina de Aragón. The range of activity concentrations for uranium series had a maximum value for ^{210}Pb of 63 ± 10 Bq kg^{-1} and a minimum value of 9.65 ± 0.46 Bq kg^{-1} for ^{214}Bi. The range of activity concentrations for thorium series was between 26.7 ± 1.1 Bq kg^{-1} for ^{228}Ac and 4.79 ± 0.30 Bq kg^{-1} for ^{208}Tl. Activity concentration of ^{226}Ra was higher than the one of ^{234}Th in samples 1 and 2, while in the rest they maintained the expected ratio of 1. Activity concentrations of ^{40}K varied between 189.4 ± 9.2 Bq kg^{-1} and 428 ± 19 Bq kg^{-1}. ^{235}U activity concentrations were below the lower limit of detection in all cases. Furthermore, ^{137}Cs was detected in 3 samples. ^{232}Th/^{238}U ratio in the samples from the inner courtyard of the castle (samples 1, 2 and 3) was 1.2, whilst the value obtained for the remaining samples was 0.75.

Figure 2 shows the box-and-whisker plot for the natural radioactive series of uranium and thorium. Both series were in secular equilibrium. However, the activity concentration of ^{210}Pb in samples 10 was higher than that of the other radionuclides of the radioactive uranium series. This sample corresponds to the final part of the church wall. This behavior was also observed in sample 9, corresponding to the synagogue. The activity concentrations of ^{208}Tl were equivalent to those of ^{228}Ac and ^{212}Pb, taking into account the branching ratio of 35.94% for the disintegration of ^{212}Bi, which is the mother of ^{208}Tl [22].

Figure 3 shows the box-and-whisker plot of the ^{40}K activity concentrations of the analyzed samples, whose spread was low, as shown by the width of the 2nd and 3rd quartiles with the mean and median also being close to each other. However, 3 atypical values were found which corresponded to samples 1, 3 and 10. These values do not have a significant statistical difference since relative kurtosis and skewness values of 0.22 and 1.1 were obtained. These values must be taken with caution since the number of samples is only 10; however, they allow verifying that the atypical data would not be considered anomalous but distant from the distribution of the activity concentrations.

Table 1 Activity concentrations (Bq kg^{-1}) of samples from the historic site of Molina de Aragón

Sample	Uranium series					^{235}U	Thorium series			^{40}K	^{137}Cs
	^{234}Th	^{226}Ra	^{214}Pb	^{214}Bi	^{210}Pb		^{228}Ac	^{212}Pb	^{208}Tl		
1	19.9 ± 3.5	33.7 ± 5.3	21.2 ± 1.7	19.6 ± 1.0	24.9 ± 4.7	< 2.5	24.6 ± 1.3	25.6 ± 2.2	10.71 ± 0.75	399 ± 18	< 0.4
2	17.4 ± 3.0	28.2 ± 4.6	14.8 ± 1.3	13.67 ± 0.74	16.4 ± 3.3	< 2.2	21.2 ± 1.1	21.6 ± 1.8	9.22 ± 0.69	283 ± 13	< 0.4
3	22.6 ± 3.7	23.1 ± 4.5	16.5 ± 1.4	15.38 ± 0.86	21.3 ± 3.9	< 2.3	26.7 ± 1.1	26.6 ± 2.2	11.35 ± 0.80	189.4 ± 9.2	< 0.4
4	17.8 ± 3.0	20.2 ± 3.8	14.1 ± 1.1	12.31 ± 0.54	15.0 ± 2.9	< 1.5	11.20 ± 0.52	11.8 ± 1.0	4.88 ± 0.33	200.6 ± 9.1	< 0.4
5	14.1 ± 2.1	16.6 ± 2.9	10.94 ± 0.94	9.65 ± 0.46	13.0 ± 2.5	< 1.5	11.11 ± 0.52	11.23 ± 0.94	4.79 ± 0.30	269 ± 12	< 0.2
6	17.9 ± 2.6	17.6 ± 3.1	13.4 ± 1.0	12.85 ± 0.51	12.9 ± 2.2	< 1.2	11.43 ± 0.47	12.1 ± 1.0	4.94 ± 0.32	257 ± 11	< 0.3
7	16.9 ± 2.9	20.0 ± 3.9	13.5 ± 1.2	12.16 ± 0.81	20.8 ± 4.1	< 2.2	14.28 ± 0.71	14.7 ± 1.2	6.25 ± 0.55	300 ± 14	0.39 ± 0.16
8	17.1 ± 3.1	14.7 ± 5.9	11.5 ± 1.0	10.18 ± 0.66	24.5 ± 4.8	< 3.7	11.06 ± 0.71	12.7 ± 1.1	4.96 ± 0.42	280 ± 13	< 0.7
9	15.2 ± 2.8	15.8 ± 3.4	12.5 ± 1.0	10.80 ± 0.51	28.2 ± 4.5	< 1.5	11.65 ± 0.53	11.9 ± 1.0	5.03 ± 0.34	260 ± 12	0.500 ± 0.072
10	21.7 ± 3.7	14.8 ± 4.4	16.4 ± 1.4	15.32 ± 0.91	63 ± 10	< 2.4	14.9 ± 1.3	15.6 ± 1.4	6.51 ± 0.42	428 ± 19	2.81 ± 0.29

The uncertainties are quoted for a coverage factor k = 2

All the samples are expressed in Bq kg^{-1}

Effective dose calculation

The comparison of the effective doses calculated from the absorbed doses (expression 1) was used to verify that the sample measured in the laboratory was representative with respect to the sampled area. The reason was that the amount of sample that could be taken was less than usual in a typical soil sampling and therefore, this way, its reproducibility is ensured. Table 2 presents the calculated effective dose rates and $H^*(10)$ dose rates for the studied samples. The % overlap was in all cases greater than 20%. The overlaps indicate that both data sets are statistically the same. The result of Student's t-test and Fisher's F showed that the means were comparable ($p = 0.91$) and the variances were homoscedastic ($p = 0.63$).

Statistical grouping of samples

Cluster analysis was used to study the groupings between the experimental values of the different samples. This analysis was applied both for the activity concentrations (Fig. 4a), and for the percentages of oxides obtained by XRF (Fig. 4b). In the Fig. 4, similarities between the grouping obtained for the activity concentration of the natural radionuclides and ^{137}Cs and the obtained for the oxides determined by XRF are observed. In both cases samples from "Prao de los Judios" (samples 5, 6, 7, 8 and 9) grouped for the radiological and chemical results. Chemical analyses showed more clearly the results of the samples of the Christian ruins, although in both cases the conclusions are equivalent. Analyses show as well that the more affected samples by archaelogical works (1, 4 and 10) would be different from the rest.

Correlation between samples, their activity concentrations and chemical compositions

The correlation between the samples and their activity concentrations and chemical compositions was studied using PCA (Fig. 5). PCA represented the 96.2% of the variance of the values. The variables that allowed obtaining a KMO higher than 0.7 were: ^{208}Tl, ^{212}Pb, ^{214}Bi, ^{214}Pb, ^{228}Ac, Fe_2O_3, Al_2O_3 and ZrO_2. The vectors obtained for the variables show a high correlation between Fe_2O_3, Al_2O_3 and the natural radioactive series of thorium (^{208}Tl, ^{212}Pb and ^{228}Ac). Likewise, a correlation between the uranium series (^{214}Pb and ^{214}Bi) and ZrO_2 was observed. The scores obtained for the previous variables showed three data sets: (a) samples 4–9, (b) sample 10 and (c) samples 1–3. The set (a) would represent the samples from the "Prao de los Judíos" and set (c) the samples from the Christian zone. Sample 10 [set (b)] would be more centered in the graph, which would indicate

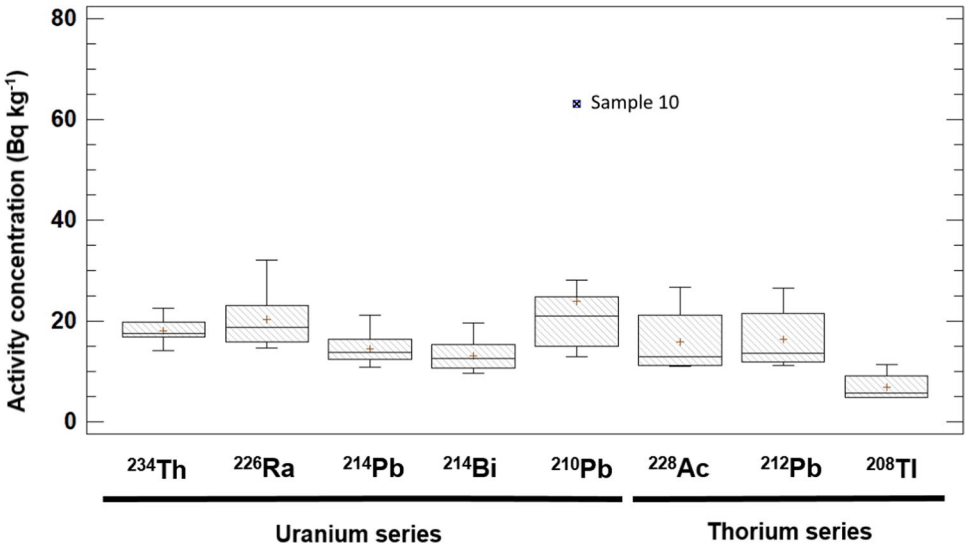

Fig. 2 Box-and-whisker plot for the activity concentrations of uranium and thorium series

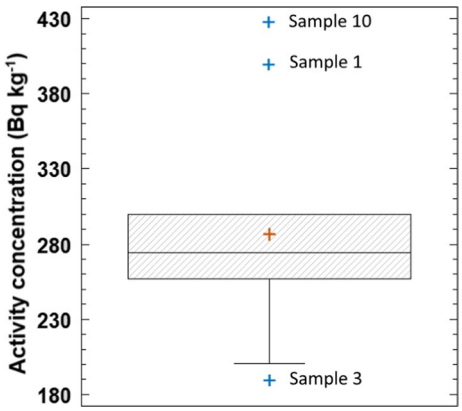

Fig. 3 Box-and-whisker plot of ^{40}K activity concentrations. The graph shows three atypical values, but within the eigenvalues of a normal distribution (kurtosis of 0.22 and skewness of 1.1)

Table 2 Absorbed dose rate at 1 m distance from the ground

Sample	$\dot{D}_{1m}$(nGy h^{-1})	E_T (μSv h^{-1})	$H^*(10)$ (μSv h^{-1})	(% Overlap)
1	36.2 ± 4.3	0.222 ± 0.027	0.210 ± 0.047	57.4
2	27.2 ± 3.4	0.167 ± 0.021	0.160 ± 0.041	51.2
3	26.3 ± 3.3	0.161 ± 0.020	0.130 ± 0.038	30.3
4	19.0 ± 2.4	0.116 ± 0.015	0.110 ± 0.033	45.5
5	20.5 ± 2.3	0.125 ± 0.014	0.160 ± 0.041	22.2
6	21.6 ± 2.2	0.132 ± 0.014	0.130 ± 0.036	38.9
7	24.3 ± 7.5	0.149 ± 0.046	0.150 ± 0.040	87
8	21.3 ± 5.6	0.131 ± 0.035	0.180 ± 0.044	23.4
9	20.9 ± 3.2	0.128 ± 0.019	0.130 ± 0.036	52.8
10	31.7 ± 5.9	0.195 ± 0.036	0.150 ± 0.040	25.6

The uncertainties are quoted for a coverage factor $k = 2$

that it does not follow the same behavior as the previous ones. Finally, the samples of set (c) would have a higher radioactive content and the percentage of oxides would also be higher than those of set (a).

Discussion

The obtained results support our hypothesis that natural gamma-emitting radionuclides and ^{137}Cs make it possible to characterize and interpret the historical footprint of the archaeological remains of the historic site of Molina de Aragón.

Activity concentration levels of ^{226}Ra, ^{232}Th (^{212}Pb) and ^{40}K were equivalent to the mean values for Spanish soils [23]. The activity concentration of ^{137}Cs indicated an alteration of the study area due to the archaeological campaigns that have been carried out. However, activity concentration for point 10 (Christian Church) was 2.81 ± 0.29 Bq kg^{-1}, which is equivalent to the terrestrial fallout and would indicate that this area has remained unchanged [6]. For points 7 and 9, activity concentrations were equivalent to the lower detection limits of the remaining points, we cannot obtain the same conclusions as in point 10.

The obtained ^{232}Th/^{238}U ratio of 1.2 for samples 1, 2 and 3, corresponding to the inner courtyard of the castle, indicated the presence of granitic materials in the construction of the castle structure [24]. However, in the remaining samples, a ratio of 0.8 was obtained, which could reflect the use of other construction materials such as brick and plaster [25]. Likewise, the activity concentration of ^{226}Ra in samples 1 and 2 (visually verified clayey appearance) was higher than the one of the other radionuclides of the

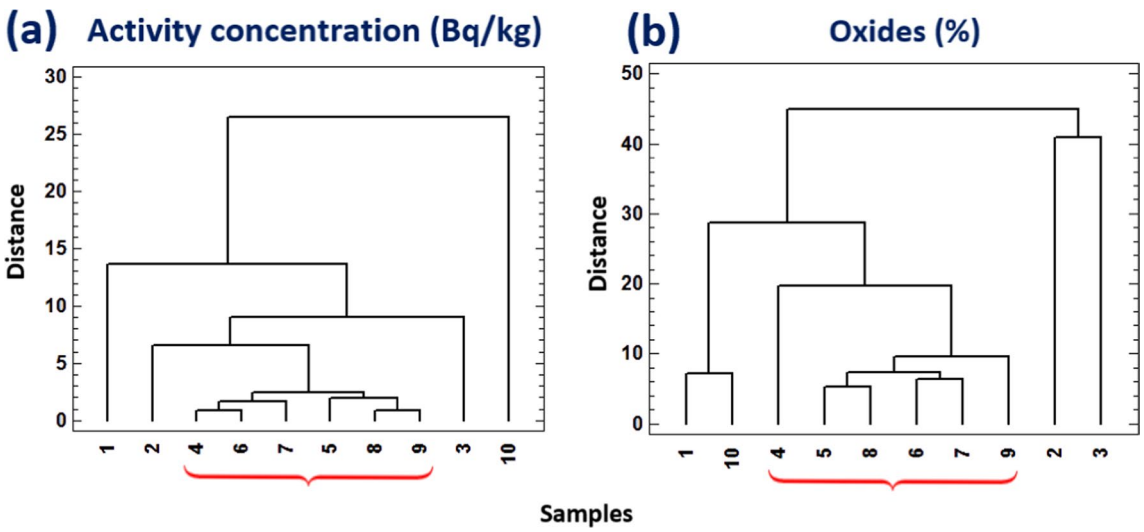

Fig. 4 Cluster analysis plot for the studied samples: **a** groupings obtained for the activity concentration of the results of the natural radioactive series, ^{40}K and ^{137}Cs (Table 2); and **b** percentage of oxides (Table A1 of the Supporting Information). The red key classifies the samples taken in the "Prao de los Judíos"

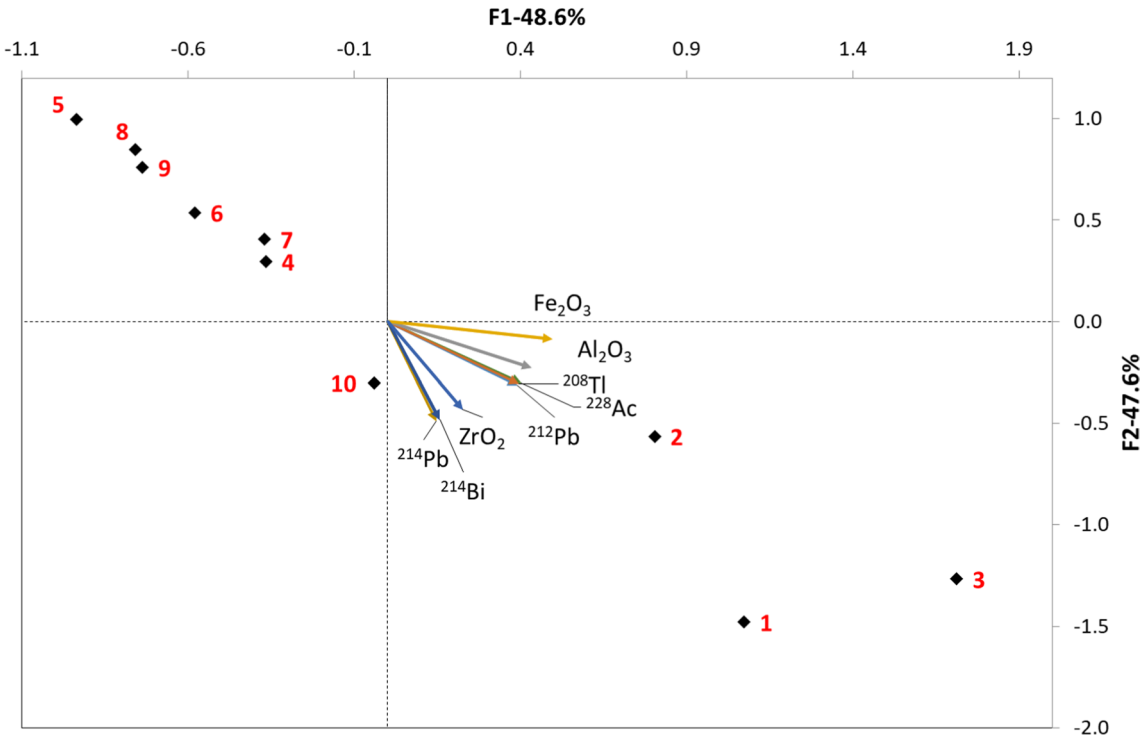

Fig. 5 HJ-Biplot graph with the representation of the variables correlation (vectors that start from the 0.0 coordinate) and the scores obtained for the different samples taken in "Molina de Aragón"

natural radioactive series of uranium. This ^{226}Ra enrichment is typically given in the presence of clay, as has been observed in previous studies [26]. The hypothesis that could be proposed is that the ^{226}Ra from the eroded granite of the walls has been retained in the clay of the soil. This behavior is consistent with the results obtained in [27] in which the radiological content was found to be higher in the fine or loose fraction of the granite.

Activity concentration of ^{210}Pb in sample 10 would indicate a value of ^{210}Pb in excess, or not supported by the radioactive

uranium series ($^{210}Pb_{ex}$) of 47 Bq kg^{-1}. The presence of $^{210}Pb_{ex}$ is related to slightly altered soils in which ^{210}Pb is generated by the disintegration of ^{222}Rn, and accumulates. $^{210}Pb_{ex}$ is also related to the concentration of ^{137}Cs [28]. The values obtained in sample 10 are consistent with this behavior and the contribution of $^{210}Pb_{ex}$ could be due to the presence of granite on the walls of the structure of the Christian church.

The effective dose rates obtained in-situ are equivalent to those deduced from the activity concentration of the gamma emitters present in the analyzed samples from the study area. The absorbed and effective dose rate levels are consistent with those obtained in previous studies in the Iberian Peninsula [29]. This finding shows that the samples analyzed in the laboratory by gamma spectrometry were representative of the areas where they were sampled.

The groupings obtained for the gamma spectrometry results (Fig. 4a) and the chemical composition obtained by XRF (Fig. 4b), were equivalent. In both cases, a clear grouping of the samples from the "Prao de los Judíos" is observed. In the case of the samples from the Christian zone, a grouping of samples 2 and 3 was observed, which was clearer for the clusters obtained for the chemical composition (percentage of oxides). Samples 1, 4 and 10 that would be most affected by the archaeological works were not grouped for these two groups described.

Finally, HJ-Biplot graph allowed to clearly observe the findings described above. The relationships of the variables showed a relationship between the natural radioactive series of thorium (^{208}Tl, ^{212}Pb and ^{228}Ac), and to a lesser extent with the uranium one (^{214}Pb and ^{214}Bi), with Fe_2O_3 and Al_2O_3, which was already found in previous works on granites [27]. This association may be due to the presence of biotites ($K(Mg,Fe)_3(AlSi_3O_{10})(OH)_2$), chlorites ($(Mg,Fe)_3(Si,Al)_4O_{10}(OH)_2 \cdot (Mg,Fe)_3(OH)_6$) and siderophyllites ($KFe_{22} + Al(Al_2Si_2O_{10})(OH)_2$) [30–32]. On the other hand, another correlation was observed between the radioactive series of uranium (^{214}Pb and ^{214}Bi), and to a lesser extent with the thorium series (^{208}Tl, ^{212}Pb and ^{228}Ac), with Zr_2O, which reflects the well-known relationship between zirconite and the radioactive series of uranium and thorium [32]. The scores obtained for the samples showed 3 sets of samples: (a) those from the "Prao de los Judíos" area, (b) samples alterated due to archaeological works and (c) samples from the Christian area. In the case of the samples from the "Prao de los Judíos", the results reflected the use of the materials described above (bricks and filling). However, samples 1–3 from the Christian ruins area, would show the use of granitic materials that is reflected by both, their chemical and radiological properties. In the case of sample 10 and to a lesser extent sample 4, the results show that they did not belong to none of the two groups described and, therefore, they would be mixed by the archaeological works in the study area.

Conclusions

The physiochemical characteristics of the natural gamma-emitting radionuclides and ^{137}Cs, as well as chemical composition, have made it possible to classify the different areas of the historic site of Molina de Aragón. The statistical study applied to the analyzed samples distinguished the area with Jewish influence ("Prao de los Judios") from the area with Christian influence (Church and inner courtyard of the Castle). ^{137}Cs and $^{210}Pb_{ex}$ allowed to identify the less altered areas of the historical assemblage. The dose rates obtained were equivalent to the radioactive background of the area.

The relationships found with the HJ-Biplot graph clearly differentiated the samples based on the scores obtained with the factors that provided a KMO > 0.7. On the one hand, a relationship between Fe_2O_3 and Al_2O_3 with the radioactive thorium series (^{208}Tl, ^{212}Pb and ^{228}Ac) and ZrO_2 with the uranium series (^{214}Pb and ^{214}Bi) was obtained. Samples with the highest radioactive content and with the greatest granite presence were those from the Christian castle complex. However, samples obtained in the "Prao de los Judíos" showed a lower contribution of these variables. The most mixed samples by the archaeological works were more centered in the HJ-Biplot graph.

This work has shown that it is possible to characterize an archaeological area solely with the information provided by gamma spectrometry. Moreover, it is not necessary to search for high levels of radioactivity to study a site, but to interpret the information provided by natural radionuclides together with ^{137}Cs. Although man has tried to leave his mark on time with great architectural constructions, something as small as uranium and thorium atoms, disintegration by disintegration, will always teach him and show him the true rhythm of history.

Supplementary Information The online version contains supplementary material available at https://doi.org/10.1007/s10967-022-08708-0.

Acknowledgements This study has been funded by the ARCHEOMEDTAL project of the University of Granada. The authors J.A. Suárez-Navarro and V.M. Expósito-Suárez are grateful for the support of CIEMAT for the internal project 353-M_CU_PILAR. Authors also want to thank Professor Begoña Artiñano Rodríguez de Torres for her support in achieving this work.

Funding Open Access funding provided thanks to the CRUE-CSIC agreement with Springer Nature.

Declarations

Conflict of interest The authors declare that they have no conflict of interest.

References

1. Gener M, Montero-Ruiz I, Murillo-Barroso M, Manzano E, Vallejo A (2014) Lead provenance study in medieval metallic materials from Madinat al-Zahra (Medina Azahara, Córdoba). J Archaeol Sci 44:154–163. https://doi.org/10.1016/j.jas.2014.01.029
2. Suárez-Navarro JA, Moreno-Reyes AM, Gascó C, Alonso MM, Puertas F (2020) Gamma spectrometry and LabSOCS-calculated efficiency in the radiological characterisation of quadrangular and cubic specimens of hardened Portland cement paste. Radiat Phys Chem 171:108709. https://doi.org/10.1016/j.radphyschem.2020.108709
3. Tzortzis M, Tsertos H, Christofides S, Christodoulides G (2003) Gamma radiation measurements and dose rates in commercially-used natural tiling rocks (granites). J Environ Radioact 70(3):223–235. https://doi.org/10.1016/s0265-931x(03)00106-1
4. Ivanovich M, Harmon RS (1992) Uranium-series disequilibrium: applications to earth, marine, and environmental sciences, 2nd edn. Clarendon Press, Oxford
5. Cowart J, Burnett W (1994) The distribution of uranium and thorium decay-series radionuclides in the environment—a review. J Environ Qual 23(4):651–662. https://doi.org/10.2134/jeq1994.00472425002300040005x
6. Ritchie JC, McHenry JR (1990) Application of radioactive fallout Cesium-137 for measuring soil erosion and sediment accumulation rates and patterns: a review. J Environ Qual 19(2):215–233. https://doi.org/10.2134/jeq1990.00472425001900020006x
7. Ruiz GG-C, Banerjea RY, Brown AD, Pluskowski AG (2016) Molina de Aragón: archaeological investigations of environmental change on the frontiers of medieval Iberia. ANTIQUITY
8. Be M, Chisté V, Dulieu C, Kellett M, Mougeot X, Arinc A, Chechev V, Kuzmenko N, Kibédi T, Luca A (2016) Table of radionuclides (Vol. 8-A= 41 to 198). Bureau International Des Poids et Mesures (BIPM), Sèvres
9. Suárez-Navarro JA, Gascó C, Alonso MM, Blanco-Varela MT, Lanzon M, Puertas F (2018) Use of Genie 2000 and Excel VBA to correct for γ-ray interference in the determination of NORM building material activity concentrations. Appl Radiat Isot 142:1–7. https://doi.org/10.1016/j.apradiso.2018.09.019
10. Suarez-Navarro JA, Pujol L, Suarez-Navarro MJ, Arana M, Hernáiz G (2019) A method for gamma background subtraction using visual basic for applications code with Microsoft excel. J Radioanal Nucl Chem 319(3):1159–1163. https://doi.org/10.1007/s10967-018-06411-7
11. UNE IE (2017) UNE-EN ISO/IEC 17025:2017. General requirements for the competence of testing and calibration laboratories
12. Saito K, Jacob P (1995) Gamma ray fields in the air due to sources in the ground. Radiat Prot Dosim 58(1):29–45
13. Taskin H, Karavus M, Ay P, Topuzoglu A, Hidiroglu S, Karahan G (2009) Radionuclide concentrations in soil and lifetime cancer risk due to gamma radioactivity in Kirklareli, Turkey. J Environ Radioact 100(1):49–53. https://doi.org/10.1016/j.jenvrad.2008.10.012
14. Kragten J (1995) A standard scheme for calculating numerically standard deviations and confidence intervals. Chemom Intell Lab Syst 28(1):89–97. https://doi.org/10.1016/0169-7439(95)80042-8
15. Kragten J (1994) Tutorial review. Calculating standard deviations and confidence intervals with a universally applicable spreadsheet technique. Analyst 119(10):2161–2165. https://doi.org/10.1039/an9941902161
16. Méndez-Ramírez I, Moreno-Macías H, Gómez-Humarán IM, Murata C (2014) Conglomerados como solución alternativa al problema de la multicolinealidad en modelos lineales. Cienc Clín 15(2):39–46. https://doi.org/10.1016/j.cc.2015.08.002
17. Dziuban CD, Shirkey EC (1974) When is a correlation matrix appropriate for factor analysis? Some decision rules. Psychol Bull 81(6):358–361. https://doi.org/10.1037/h0036316
18. Zaiontz C (2020) Real statistics using excel. www.real-statistics.com
19. Carrasco G, Molina J-L, Patino-Alonso M-C, Castillo MDC, Vicente-Galindo M-P, Galindo-Villardón M-P (2019) Water quality evaluation through a multivariate statistical HJ-Biplot approach. J Hydrol 577:123993. https://doi.org/10.1016/j.jhydrol.2019.123993
20. Expósito-Suárez VM, Suárez-Navarro JA, Benavente JF, Aragón P, Mora JC (2022) Radiological characterization of a uranium glass collectible by gamma spectrometry. Radiat Phys Chem 199:110299. https://doi.org/10.1016/j.radphyschem.2022.110299
21. Sanjuan MA, Suarez-Navarro JA, Argiz C, Barragan M, Hernaiz G, Cortecero M, Lorca P (2022) Radiological characteristics of carbonated Portland cement mortars made with GGBFS. Materials (Basel). https://doi.org/10.3390/ma15093395
22. Kobya Y, Taşkın H, Yeşilkanat CM, Varinlioğlu A, Korcak S (2015) Natural and artificial radioactivity assessment of dam lakes sediments in Çoruh River, Turkey. J Radioanal Nucl Chem 303(1):287–295. https://doi.org/10.1007/s10967-014-3420-7
23. UNSCEAR (2000) Sources and effects of ionizing radiation. UNSCEAR 2000 report to the General Assembly, with scientific annexes. Volume I: Sources. United Nations Scientific Committee on the Effects of Atomic Radiation
24. Daza Pardo E (2015) Técnicas y materiales de la construcción fortificada altomedieval en el centro de la Península Ibérica: métodos de análisis a través de la arqueología y la historia de la construcción (in Spanish). Universidad Politécnica de Madrid
25. Freire-Lista DM (2021) The forerunners on heritage stones investigation: historical synthesis and evolution. Heritage 4(3):1228–1268
26. Vandenhove H, Van Hees M (2007) Predicting radium availability and uptake from soil properties. Chemosphere 69(4):664–674. https://doi.org/10.1016/j.chemosphere.2007.02.054
27. Suárez-Navarro JA, Alonso MdM, Gascó C, Pachón A, Carmona-Quiroga PM, Argiz C, Sanjuán MÁ, Puertas F (2021) Effect of particle size and composition of granitic sands on the radiological behaviour of mortars. Bol Soc Esp Cerám Vidrio. https://doi.org/10.1016/j.bsecv.2021.05.001
28. Mabit L, Benmansour M, Walling DE (2008) Comparative advantages and limitations of the fallout radionuclides 137Cs, 210Pbex and 7Be for assessing soil erosion and sedimentation. J Environ Radioact 99(12):1799–1807. https://doi.org/10.1016/j.jenvrad.2008.08.009

29. Quindós Poncela LS, Fernández PL, Gómez Arozamena J, Sainz C, Fernández JA, Suarez Mahou E, Martin Matarranz JL, Cascón MC (2004) Natural gamma radiation map (MARNA) and indoor radon levels in Spain. Environ Int 29(8):1091–1096. https://doi.org/10.1016/S0160-4120(03)00102-8
30. Puziewicz J, Johannes W (1990) Experimental study of a biotite-bearing granitic system under water-saturated and water-undersaturated conditions. Contrib Miner Petrol 104(4):397–406. https://doi.org/10.1007/BF01575618
31. David RW, Hans PE (1965) Stability of biotite: experiment, theory, and application. Am Miner 50(9):1228–1272
32. Albee AL (1965) Distribution of Fe, Mg, and Mn between garnet and biotite in natural mineral assemblages. J Geol 73(1):155–164. https://doi.org/10.1086/627051